Effect of Varying Prior Information in Axillary 2D Microwave Tomography

Matteo Savazzi*, Olympia Karadima†, João M. Felício‡§, Carlos A. Fernandes‡,
Panagiotis Kosmas†¶, Raquel C. Conceição*
*Instituto de Biofísica e Engenharia Biomédica, Faculdade de Ciências, Universidade de Lisboa, Campo Grande, 1749-016 Lisbon, Portugal,
mlsavazzi@fc.ul.pt, rcconceicao@fc.ul.pt
†Faculty of Natural and Mathematical Sciences, King's College London, Strand, London WC2R 2LS, London, UK,
olympia.karadima@kcl.ac.uk, panagiotis.kosmas@kcl.ac.uk
‡Instituto de Telecomunicações, Instituto Superior Técnico (IST), Universidade de Lisboa, 1049-001 Lisbon, Portugal,
joao.felicio@lx.it.pt, carlos.fernandes@lx.it.pt
§Centro de Investigação Naval (CINAV), Escola Naval, 2810-001 Almada, Portugal
¶Metamaterials Inc., Dartmouth, Canada, NS B2Y 4M9,
panagiotis.kosmas@metamaterial.com

***Abstract*—We numerically assess the potential of microwave tomography (MWT) for the detection and dielectric properties estimation of axillary lymph nodes (ALNs), and we study the robustness of our system using prior information with varying levels of accuracy. We adopt a 2-dimensional MWT system with 8 antennas (0.5-2.5 GHz) placed around the axillary region. The reconstruction algorithm implements the distorted Born iterative method. We show that: (i) when accurate prior knowledge of the axillary tissues (fat and muscle) is available, our system successfully detects an ALN; (ii) $\pm 30\%$ error in the prior estimation of fat and muscle dielectric properties does not affect image quality; (iii) $\pm 7mm$ error in muscle position causes slight artifacts, while $\pm 14mm$ error in muscle position affects ALN detection. To the best of our knowledge, this is the first paper in the literature to study the impact of prior information accuracy on detecting an ALN using MWT.**

***Index Terms*—axillary lymph node imaging, breast cancer, distorted Born iterative method (DBIM), microwave tomography, prior information.**

I. Introduction

In the context of breast cancer diagnosis and treatment planning, the diagnosis of axillary lymph nodes (ALNs) is fundamental as the status (healthy or pathological) of these organs is essential to determine cancer staging before making therapeutical decisions [1].

In developed countries, the state-of-the-art method for ALN diagnosis is sentinel lymph node biopsy (SLNB), which consists of the surgical excision and histological examination of the first regional node (or nodes) to drain the primary tumour. However, SLNB is an invasive procedure which often leads to longer patient recovery, risk of infection and lymphoedema [2], [3]. Standard imaging modalities, such as Magnetic Resonance Imaging (MRI) or the combination of Positron Emission Tomography and Computed Tomography (PET-CT), are currently used as alternatives to avoid (when possible) SLNB, but they present some limitations: MRI has low specificity, while PET-CT has low sensitivity; both of them are associated to high costs and, PET-CT is associated to radiation exposure. Thus, there is a clinical need for an alternative technology which can diagnose ALNs non-invasively, and low costs.

The possibility of imaging ALNs using microwave imaging (MWI) is under study in our research group [4], [5], [6], [7], and other authors in the literature considered such possibility [8]. However, axillary MWI presents considerable challenges if compared to other medical-MWI applications: here, given the morphology of the axilla, antennas cannot be placed in a circular configuration, but only in a limited arc around the area of interest ($\approx 90°$), significantly limiting the information available for image reconstruction. In addition, we already argued [6] that the presence of muscle tissue near the ALNs hinders the detection of ALN. Hence, in order validate MWI as a viable imaging modality for ALN diagnosis, it is clear that research efforts should focus on the mitigation of the influence of the muscle in imaging algorithms.

Microwave tomography (MWT) algorithms explore available prior information, incorporating a guess of the dielectric map of the investigated region (*initial guess*) into the reconstruction algorithm. This practice has been suggested to significantly improve image quality in breast MWT [9]. Authors in [10] quantified the impact of errors in prior information on image quality in the case of breast MWT.

In this paper, we assess the imaging performance of MWT for the detection and dielectric properties estimation of ALNs, using the distorted Born iterative method (DBIM). In particular, we aim to: i) study if DBIM can detect and estimate the dielectric properties of an ALN when prior knowledge of surrounding tissues is available; ii) study the robustness of the algorithm to uncertainties/errors in the prior information of surrounding tissues (notably, muscle dielectric properties and its position). To do so, we consider a 2-dimensional (2D)

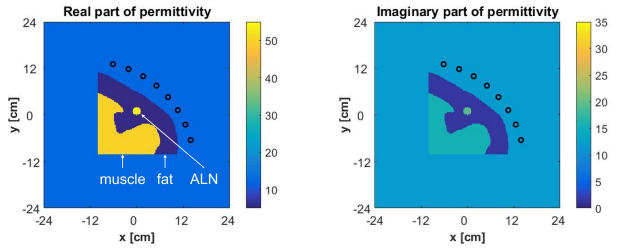

(a) (b)

Fig. 1. 2D tomographic setup used to assess axillary microwave tomography: 8 point-source antennas (black circles) are placed in a quarter-circular configuration around the axillary region, which is composed of three tissues: fat, muscle, and axillary lymph node (ALN). The figure colors define the complex permittivity of axillary tissues at 1.5 GHz **(a)** Real part of permittivity; **(b)** Imaginary part of permittivity.

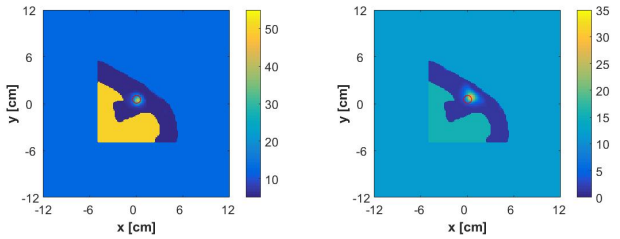

(a) (b)

Fig. 2. Benchmark: reconstructed complex permittivity for the case where the *initial guess* represents the exact anatomy and dielectric properties of the tissues surrounding the ALN. The inner red circle shows the actual position of the ALN. **(a)** Real part of permittivity; **(b)** Imaginary part of permittivity. Frequency = 1.5 GHz.

MWT simulation to image an axial slice of the axillary region. This allows us to study the impact of prior information in ideal conditions, without measurement and model mismatch errors. Moreover, the 2D model has the advantage of speeding up the computation time of the DBIM, which is particularly relevant considering that DBIM solves an EM problem (forward solution) at each iteration. To the best of our knowledge, this is the first paper in the literature to study the impact of prior information accuracy on detecting an ALN using MWT.

II. Methods

We used a 2D axial representation of the axillary region anthropomorphic model that we developed in [5], where we included a circular ALN (radius of 5mm). Given the marginal influence of lung and bone on the E-field coupling inside the axillary region [5], we decided not to consider them in our study. As a result, the adopted axillary model consists of three tissue types: fat, muscle, and ALN. The anatomy and the dielectric properties (at 1.5 GHz) of the axillary model can be visualised in Fig. 1.

The setup is represented in Fig. 1, and considers eight antennas facing the axillary region in a quarter-circular array configuration. Antennas are point sources that generate wide-band Gaussian pulses centered at 1.5 GHz in a transverse magnetic (TM) configuration, and are immersed in a lossy immersion liquid made of 90% Glycerol-water mixture (Glycerol 90). The complex permittivity of Glycerol 90 is $\epsilon_r = 14.3 - 13.2j$ at 1.5 GHz. We sampled the E-field at the sources in 11 equally-spaced frequency points covering the 0.5-2.5 GHz band.

We produced simulation data using the finite-difference time-domain (FDTD) EM-solver with a convolutional perfectly matched layer (CPML) boundary condition, using a 0.5x0.5mm^2 mesh size. To solve the nonlinear inverse EM scattering problem, we employed the general framework of the DBIM [11], combined with the two-step iterative shrinkage/thresholding (TwIST) algorithm [12] to solve the linearised system of equations at each iteration. The adopted algorithm was originally proposed for 2D breast MWI [13], and experimentally tested in [14], [15]. Regarding the EM-solver used by the inversion algorithm, we adopted the same FDTD implementation used for the generation of the data. We note that, to avoid the so called "inverse crime", we used a 2x2mm^2 mesh size, which differs from the size of the mesh used for data generation. We then calibrated our data as proposed in [16], considering the axillary model without ALN as a reference scenario for calibration.

We used a frequency hopping approach, which firstly reconstructs lower frequencies, and uses the resulting dielectric map as the *initial guess* to the subsequent (higher) frequencies. This allows to initially exploit the stabilizing effect of lower frequencies, together with the finer resolution of higher frequencies, resulting in an enhanced imaging performance as reported in [13], [14], [15]. We considered 11 equally-spaced frequency points between 0.5 and 2.5 GHz, and we performed 50 DBIM-TwIST iterations at each frequency. We assigned different heterogeneous dielectric maps as the *initial guess* of the DBIM algorithm at 0.5 GHz.

Firstly, to investigate if DBIM can detect and estimate the ALN position and properties, we defined an *initial guess* which consisted of a heterogeneous dielectric map, representing the investigated model without the target. We considered this case as a benchmark, as it represents the ideal case, where all the axillary tissues (except the target) are known *a priori*. Secondly, to evaluate the robustness to errors in the *initial guess*, we introduced errors in the initial estimation of (i) dielectric properties of the axillary tissues, and (ii) muscle/fat interface position.

III. Results

Fig. 2 presents the imaging results for the benchmark case where the *initial guess* represents the exact anatomy and dielectric properties of the tissues surrounding the ALN. We observe that the ALN is detected in its correct position, with good estimation of the real part of permittivity, and a slight underestimation of the imaginary part of permittivity.

A. Robustness to errors in dielectric properties

In order to study the effect of errors in the initial estimation of the background dielectric properties, we examined the cases where the dielectric properties of fat are perturbed in the range

between -30% and +100%, and the dielectric properties of muscle are perturbed by $\pm 30\%$. We did not introduce errors in the permittivity of the immersion liquid, as this is not patient-dependent and is known ahead of each measurement. Fig. 3 (a, b) reports the reconstruction results for the case where the dielectric properties of both fat and muscle are overestimated by +30%. The images show that, despite the introduced error in the dielectric properties prior knowledge, the ALN is detected in its correct position, and no noticeable differences are visible when comparing these results with the benchmark case in Fig. 2. We also report that we observed similar results when initially underestimating the dielectric properties of fat and muscle tissue by -30%. For the sake of brevity, we did not report such results in the present paper, but we will during our presentation.

To further investigate the robustness of our algorithm to errors in the prior estimation of dielectric properties, we studied the case were the dielectric properties of fat are overestimated by +100%, and the dielectric properties of muscle are underestimated by -30%. Fig. 3 (c, d) reports the reconstruction results. The images show that the ALN is detected in its correct position, but with a reduced contrast, which is particularly evident in the imaginary part of the permittivity. We report that similar results were obtained when introducing a +100% error in fat and a +30% error in muscle dielectric properties. We believe that these are good results as it is reasonable to consider the last two described cases as "worst case scenarios". In light of the physiological variability of biological tissues dielectric properties among individuals, we are confident that potential errors in dielectric properties will be lower than 100% for fat and lower than 30% for muscle tissues.

B. Robustness to errors in fat/muscle interface

In order to study the effect of errors in the initial estimation of the position of fat/muscle interface, we translated the interface along the vectors represented in Fig. 4 (left column). As a result, we considered four different *initial guesses*, corresponding to the following translation vectors with respect to the true position of the muscle: -14mm, -7mm, +7mm, +14mm; where a negative translation indicates a movement toward lower x and y coordinates in Fig. 4 (larger fat region in the *initial guess*), and a positive translation indicates a movement toward larger x and y coordinates in Fig. 4 (smaller fat region in the *initial guess*).

Fig. 4 reports the results for the four cases. Fig. 4 (c,d) and Fig. 4 (e,f) suggest that the detection of the ALN is still clear when translating the fat/muscle interface by $\pm 7mm$. The image quality deteriorates when the error in prior information increases to $\pm 14mm$. Fig 4 (a, b) shows that the ALN can be obscured by muscle - based on the imaginary part - when the *initial guess* of the fat/muscle interface is translated by -14mm with respect to its true position; while Fig 4 (g,h) shows that the ALN position is not well estimated in the case where the fat/muscle interface is initially translated by +14mm with respect to its true position.

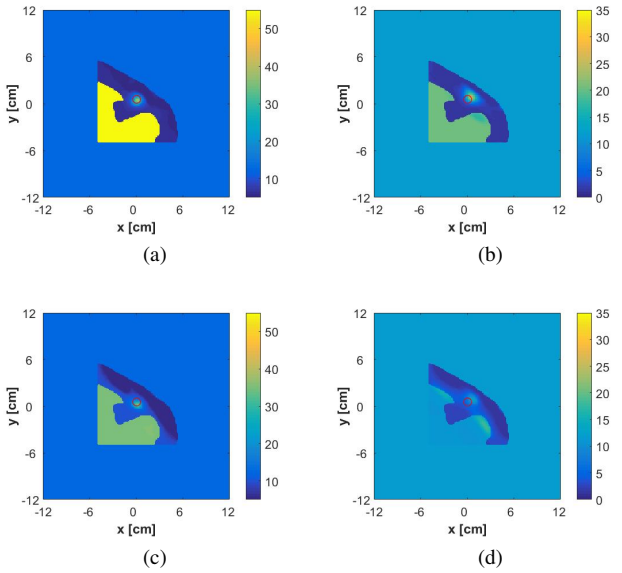

Fig. 3. Reconstructed complex permittivity for the cases where errors are introduced in the *initial guess* of the dielectric properties of fat and muscle tissues. The error in the initial estimation of dielectric properties is **(a, b)** +30% for both fat and muscle; **(c, d):** -30% for muscle and +100% for fat. The red circle shows the actual position of the ALN. **Left column:** Real part of permittivity; **Right column:** Imaginary part of permittivity. Frequency = 1.5 GHz.

C. Robustness to errors in both dielectric properties and fat/muscle interface

As a final test, we studied the effect of errors in the initial estimation of the position of fat/muscle interface when an error in the initial estimation of dielectric properties simultaneously occurs. To do so, we considered the same four cases studied in Sec. III-B, and added +30% error to the initial estimation of dielectric proprieties. As in Sec. III-B, we applied the following translations to the initial guess of the fat/muscle interface with the respect to its true position: -14mm, -7mm, +7mm, +14mm. Fig. 5 reports the results for the four cases. If comparing Fig. 5 to Fig. 4, we notice that no significant differences can be observed when adding a +30% error in the initial estimation of dielectric properties. Similar results were observed for the cases where we introduced a -30% error in the initially guessed dielectric properties. These results suggest that - even when errors in fat/muscle interface occur - errors in dielectric properties prior estimation ($\pm 30\%$) do not affect the overall quality of the reconstructed image.

IV. Conclusions and Future Work

We numerically assessed - for the first time in the literature - the possibility of detecting ALNs using MWT, and we investigated the robustness of the DBIM algorithm to errors in prior information of axillary tissues surrounding the ALN.

We observed that, when prior knowledge of muscle position is available, the ALN is detected in its correct position, with a good estimation of the real part of permittivity, and an overestimation of the imaginary part of permittivity. In

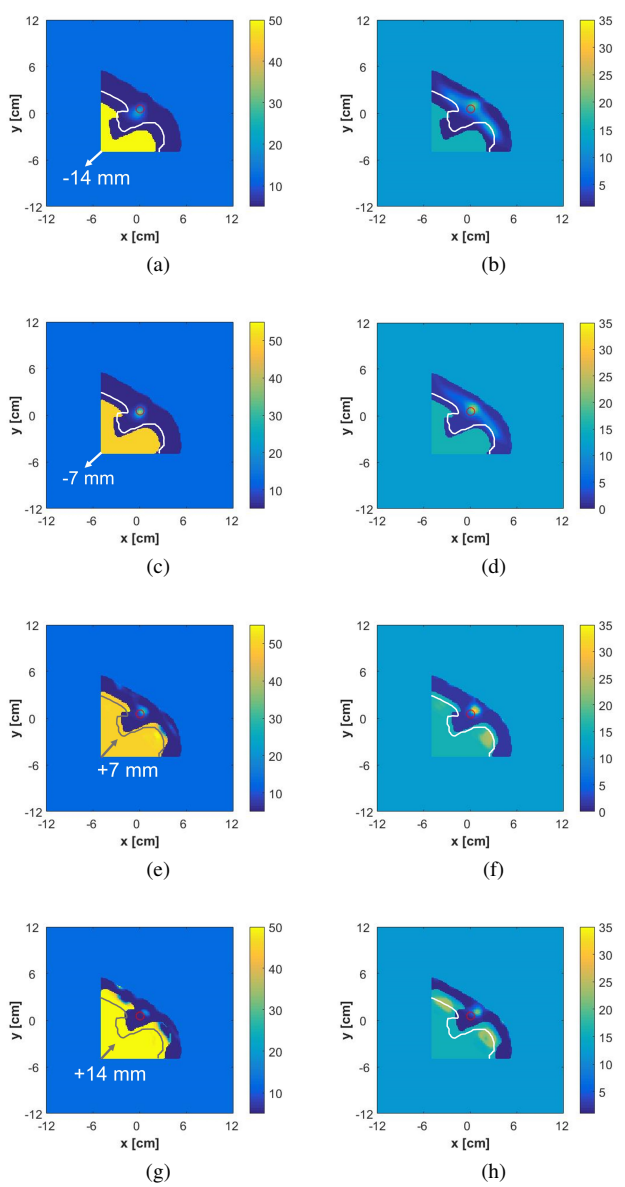

Fig. 4. Reconstructed complex permittivity for the cases where the position of the *initial guess* of the fat/muscle interface is translated with respect to its true position. The translation vector is indicated (for each case) by the arrow in the left column. The direction of the translation vector bisects the first and third quadrants of the reference system. The modulus of the translation vector is: **a, b** -14mm, **c, d** -7mm; **e, f** +7mm; **g, h** +14mm. The white/grey line traces the true fat/muscle interface. The red circle shows the actual position of the ALN. **Left column:** real part of permittivity; **right column:** imaginary part of permittivity. Frequency = 1.5 GHz.

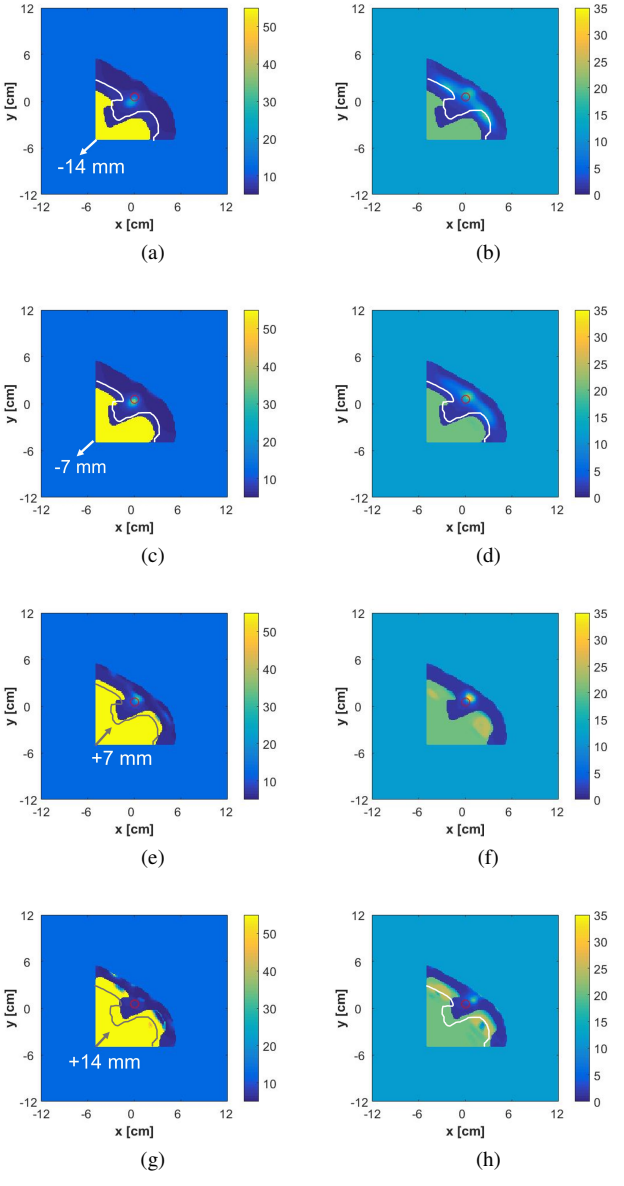

Fig. 5. Reconstructed complex permittivity for the cases where the errors in the *initial guess* involve both the dielectric properties of fat and muscle tissues and the position of the fat/muscle interface (translation with respect to its true position). The error in dielectric properties is a +30% overestimation for all cases. The error in fat/muscle interface position is indicated (for each case) by the translation vector in the left column; the modulus of the translation vector is: **a, b** -14mm, **c, d** -7mm; **e, f** +7mm; **g, h** +14mm. The white/grey line traces the true fat/muscle interface. The red circle shows the actual position of the ALN. **Left column:** real part of permittivity; **right column:** imaginary part of permittivity. Frequency = 1.5 GHz.

addition, we showed that results do not significantly change when a $\pm$ 30% error occurs in the initial estimation of the dielectric properties of the axillary tissues surrounding the target; the ALN is detected with less contrast in the case where the error in prior estimation of dielectric properties is +100% for fat and $\pm$30% for muscle. We consider this a good result, which suggests robustness of our algorithm to errors in the initial estimation of the dielectric properties. Regarding the robustness of the algorithm to errors in the estimation of the muscle position, we demonstrated that, for a positioning error of $\pm 7mm$, the detection of the ALN is still acceptable; while for $\pm 14mm$ error, the image quality deteriorates, even if the ALN remains visible.

In conclusion, this study suggests that prior knowledge of muscle position is fundamental for the detection and dielectric properties estimation of ALNs. Future work on axillary MWI should focus on understanding how such knowledge can be inferred *a priori*, bearing in mind that errors in the initial estimation of muscle/fat interface should be minimised. One strategy may reside in using radar-MWI algorithms to firstly estimate the muscle position, and then integrate this information into MWT reconstruction - an analogous approach has been proposed in the literature for breast MWI [17]. A second strategy may be to use patient-specific information (e.g. body mass index) which correlates with the amount of fat laying between skin and muscle surface.

ACKNOWLEDGMENT

This work was supported by the EMERALD project funded from the European Union's Horizon 2020 research and innovation programme under the Marie Skłodowska-Curie grant agreement No. 764479.

This work is also supported by Fundação para a Ciência e a Tecnologia-FCT, FCT/MEC (PIDDAC) under the Strategic Programme UIDB/00645/2020, and UIDB/50008/2020.

REFERENCES

[1] G. H. Lyman, A. E. Giuliano, M. R. Somerfield, A. B. Benson III, D. C. Bodurka, H. J. Burstein, A. J. Cochran, H. S. Cody III, S. B. Edge, S. Galper *et al.*, "American Society of Clinical Oncology Guideline Recommendations for Sentinel Lymph Node Biopsy in Early-Stage Breast Cancer," *Journal of Clinical Oncology*, vol. 23, no. 30, pp. 7703–7720, 2005.

[2] H. Rahbar, S. C. Partridge, S. H. Javid, and C. D. Lehman, "Imaging axillary lymph nodes in patients with newly diagnosed breast cancer," *Current problems in diagnostic radiology*, vol. 41, no. 5, pp. 149–158, 2012.

[3] G. H. Lyman, M. R. Somerfield, L. D. Bosserman, C. L. Perkins, D. L. Weaver, and A. E. Giuliano, "Sentinel Lymph Node Biopsy for Patients with Early-Stage Breast Cancer: American Society of Clinical Oncology Clinical Practice Guideline Update," *Journal of Clinical Oncology*, vol. 35, no. 5, pp. 561–564, 2017.

[4] R. Eleutério and R. C. Conceição, "Initial study for detection of multiple lymph nodes in the axillary region using microwave imaging," in *2015 9th European Conference on Antennas and Propagation (EuCAP)*. IEEE, 2015, pp. 1–3.

[5] M. Savazzi, S. Abedi, N. Ištuk, N. Joachimowicz, H. Roussel, E. Porter, M. O'Halloran, J. R. Costa, C. A. Fernandes, J. M. Felício *et al.*, "Development of an Anthropomorphic Phantom of the Axillary Region for Microwave Imaging Assessment," *Sensors (Basel, Switzerland)*, vol. 20, no. 17, pp. 49–68, 2020.

[6] M. Savazzi, J. R. Costa, C. A. Fernandes, J. M. Felício, and R. C. Conceição, "Numerical Assessment of Microwave Imaging for Axillary Lymph Nodes Screening Using Anthropomorphic Phantom," in *2021 15th European Conference on Antennas and Propagation (EuCAP), Dusseldorf (Germany)*. IEEE, 2021, pp. 1–4.

[7] D. M. Godinho, J. Felicio, C. A. Fernandes, and R. C. Conceicao, "Experimental evaluation of an axillary microwave imaging system to aid breast cancer staging," *IEEE Journal of Electromagnetics, RF and Microwaves in Medicine and Biology*, 2021.

[8] J. Liu and S. G. Hay, "Prospects for Microwave imaging of the Lymphatic System in the Axillary," in *2016 IEEE-APS Topical Conference on Antennas and Propagation in Wireless Communications (APWC), Cairns, QLD, Australia*. IEEE, 2016, pp. 183–186.

[9] D. Kurrant, A. Baran, J. LoVetri, and E. Fear, "Integrating prior information into microwave tomography part 1: Impact of detail on image quality," *Medical physics*, vol. 44, no. 12, pp. 6461–6481, 2017.

[10] D. Kurrant, E. Fear, A. Baran, and J. LoVetri, "Integrating prior information into microwave tomography part 2: Impact of errors in prior information on microwave tomography image quality," *Medical physics*, vol. 44, no. 12, pp. 6482–6503, 2017.

[11] W. C. Chew and Y.-M. Wang, "Reconstruction of two-dimensional permittivity distribution using the distorted born iterative method," *IEEE transactions on medical imaging*, vol. 9, no. 2, pp. 218–225, 1990.

[12] J. M. Bioucas-Dias and M. A. Figueiredo, "A new twist: Two-step iterative shrinkage/thresholding algorithms for image restoration," *IEEE Transactions on Image processing*, vol. 16, no. 12, pp. 2992–3004, 2007.

[13] Z. Miao and P. Kosmas, "Multiple-Frequency DBIM-TwIST Algorithm for Microwave Breast Imaging," *IEEE Transactions on Antennas and Propagation*, vol. 65, no. 5, pp. 2507–2516, 2017.

[14] S. Ahsan, Z. Guo, Z. Miao, I. Sotiriou, M. Koutsoupidou, E. Kallos, G. Palikaras, and P. Kosmas, "Design and experimental validation of a multiple-frequency microwave tomography system employing the dbim-twist algorithm," *Sensors*, vol. 18, no. 10, p. 3491, 2018.

[15] O. Karadima, M. Rahman, I. Sotiriou, N. Ghavami, P. Lu, S. Ahsan, and P. Kosmas, "Experimental Validation of Microwave Tomography with the DBIM-TwIST Algorithm for Brain Stroke Detection and Classification," *Sensors*, vol. 20, no. 3, p. 840, 2020.

[16] M. Ostadrahimi, P. Mojabi, C. Gilmore, A. Zakaria, S. Noghanian, S. Pistorius, and J. LoVetri, "Analysis of incident field modeling and incident/scattered field calibration techniques in microwave tomography," *IEEE Antennas and Wireless Propagation Letters*, vol. 10, pp. 900–903, 2011.

[17] A. Baran, D. J. Kurrant, A. Zakaria, E. C. Fear, and J. LoVetri, "Breast imaging using microwave tomography with radar-based tissue-regions estimation," *Progress In Electromagnetics Research*, vol. 149, pp. 161–171, 2014.